Our application to N-body calculations is only one in a range of possibilities including the calculation of radiation fields (replacing particles with sources) and self-gravitating fluid flow (cell division being governed by the complexity of the local flow pattern). Thus our technique forms a general tool for simultaneously handling a large number of long-range interactions and for concentrating computing resources locally where most needed.

We thank John Bahcall, Jeremiah Ostriker and especially Gerald Sussman for interesting discussions. Part of this work was supported by the NSF through grant PHY-8217352; P.H. is an Alfred P. Sloan Foundation fellow.

Received 16 July; accepted 1 October 1986.

1. Aarseth, S. J. in *Multiple Time Scales* (ed. Brackbill, J. U. & Cohen, B. I.) 377-418 (Academic Press, New York, 1985).
2. Hockney, R. W. & Eastwood, J. W. *Computer Simulation using Particles* (McGraw-Hill, New York, 1981).
3. Appel, A. *SIAM J. Sci. statist. Comput.* **6**, 85-103 (1985).
4. Jernigan, J. G. *I.A.U. Symp.* **113**, 275-284.
5. Porter, D. thesis, Physics Dept, Univ. California, Berkeley (1985).
6. Abelson, H., Sussman, G. J. & Sussman, J. *Structure and Interpretation of Computer Programs* (MIT Press, Cambridge, Massachusetts, 1985).

The 400-km seismic discontinuity and the proportion of olivine in the Earth's upper mantle

Craig R. Bina & Bernard J. Wood

Department of Geological Sciences, Northwestern University, Evanston, Illinois 60201, USA

The 400-km seismic discontinuity has traditionally been ascribed to the isochemical transformation of α-olivine to the β-modified-spinel structure in a mantle of peridotitic bulk composition[1-6]. It has recently been proposed[7,8] that the observed seismic velocity increase at 400 km depth is too abrupt and too small to result from a phase change in olivine but instead requires that the transition zone be chemically distinct in bulk composition from the uppermost mantle. By requiring phase relations in the Mg_2SiO_4-Fe_2SiO_4 system to be internally consistent thermodynamically, we find that the α-β transition in olivine of mantle $(Mg_{0.9}Fe_{0.1})_2SiO_4$ composition is extremely sharp, occurring over a depth interval (isothermal) of ~6 km. The magnitude of the predicted velocity increase is in agreement with that observed seismically[9,10] if the transition zone is composed of ~60–70% olivine. Thus, our results indicate that seismic velocities across the 400-km discontinuity are consistent with a transition zone of homogeneous peridotitic composition and do not require chemical stratification.

The 400-km seismic discontinuity reflects a change in elastic properties of the mantle and has been attributed to a phase transformation of olivine to a spinel-like structure at high pressures[1]. Subsequent work has given rise to a generally accepted model in which the discontinuity is attributed to such an isochemical phase change in a mantle of homogeneous olivine-rich, or peridotitic, composition[2-6]. This model has the advantage of simplicity and can be tested experimentally.

Recently, it has been suggested[7,8] that a phase transition in olivine would produce a gradual velocity increase over an appreciable depth interval—rather than the abrupt increase observed seismically—and that the magnitude of the increase would be more than twice that actually observed. It was proposed that the seismic data require the transition zone to be chemically distinct in bulk composition from the uppermost mantle, with the transition zone consisting of a pyroxene-garnet rich 'piclogite' composition containing either 16%[7] or 30%[8] olivine. The 400-km discontinuity is ascribed to either a change in chemical composition from peridotite to underlying piclogite or—if this periodotite/piclogite boundary is referred to shallower depths—to the transformation of pyroxene to a garnet-like structure.

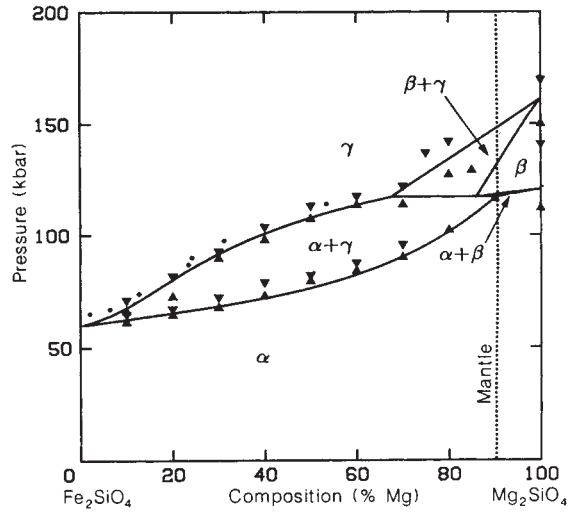

Fig. 1 Isothermal pressure-composition diagram showing calculated boundaries for olivine polymorph stability fields at 1,273 K. Also shown are experimental data points[12-14,18-20] delimiting the high-pressure stability limits of the low-pressure assemblages (▲), the low-pressure stability limits of the high-pressure assemblages (▼), and the compositions of γ phase which coexist with α phase at the indicated pressures (●). Dashed line shows $(Mg_{0.9}Fe_{0.1})_2SiO_4$ composition.

In a previous study[11], we showed that the transformation of pyroxene to a garnet structure would produce a smooth and gradual increase in seismic velocity, rather than the discontinuity observed at 400 km. In the present study, we have examined the olivine-spinel phase transitions to determine whether the observed seismic velocity variations may be attributable to such a phase change. The α-olivine to β-modified-spinel transition has been commonly represented by a broad '$\alpha+\beta$ divariant loop', a region in which both phases coexist in stable equilibrium. If this representation were accurate, the α phase would transform to the β phase in a continuous and gradual manner, and this phase change would not produce a sharp discontinuity in seismic velocity. However, the available experimental data (Fig. 1) do not constrain the width of this $\alpha+\beta$ loop, since no high-pressure experiments have yet produced both phases together in equilibrium for olivine of mantle $(Mg_{0.9}Fe_{0.1})_2SiO_4$ composition. We have used available thermoelastic and calorimetric data on the olivine polymorphs (α-olivine, β-modified-spinel, and γ-spinel) to constrain the width of the $\alpha+\beta$ divariant loop. By requiring the phase diagram for the Mg_2SiO_4-Fe_2SiO_4 system to be internally consistent thermodynamically, we have attempted to determine the sharpness and magnitude of a seismic discontinuity resulting from a phase change in olivine.

If the partial molar free energies of Mg_2SiO_4 and Fe_2SiO_4 components are known as functions of pressure, temperature, and composition, then the boundaries of the stability fields for the various phase assemblages (α, $\alpha+\beta$, β, $\beta+\gamma$ and so on) can be calculated explicitly. To compute the free-energy functions, we require knowledge of the enthalpies, entropies, volumes, and solution activities of the components in the various phases at the pressures, temperatures and compositions of interest. We used the available experimentally-measured values of the enthalpies and entropies[5,12-14], heat capacities[15], molar volumes and coefficients of thermal expansion[4], elastic moduli[16], and activity coefficients[17] for the phases and components in question. Where measured values were extremely uncertain or

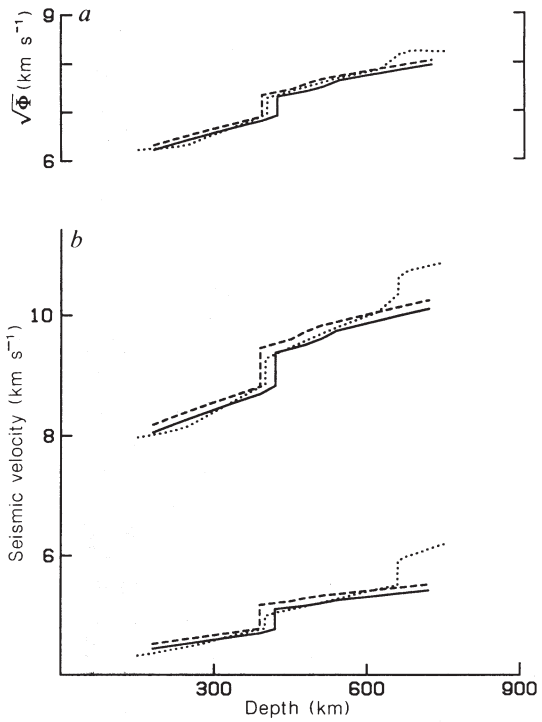

Fig. 2 *a*, Calculated bulk sound velocity ($\sqrt{\Phi}$) as a function of depth for a mantle consisting of pure olivine of $(Mg_{0.9}Fe_{0.1})_2SiO_4$ composition, along 1,700 K (dashed line) and 2,000 K (solid line) isotherms. Composite seismic profile GCA+TNA[9,10] (dotted line) is shown for comparison. *b*, Calculated P- and S-wave velocities (V_P and V_S, respectively) as functions of depth for a mantle consisting of pure olivine of $(Mg_{0.9}Fe_{0.1})_2SiO_4$ composition, along 1,700 K (dashed line) and 2,000 K (solid line) isotherms. Composite seismic profile GCA+TNA (dotted) is shown for comparison.

unavailable (such as for the metastable β-Fe_2SiO_4 component), we estimated them by formally inverting the calculation procedure and requiring the estimated values to reproduce the observed phase relations as constrained by the available synthesis data[12-14,18-20]. (Detailed discussions of the experimental data, the methods of computation and the requirements of thermodynamic consistency are presented elsewhere[21].) Using the Grüneisen thermal state equations[22] and the third-order Birch-Murnaghan isothermal state equation[23] to compute the temperature and pressure dependencies, respectively, of the molar volumes, we computed the boundaries of the stability fields in pressure-composition space for the various assemblages along the Mg_2SiO_4-Fe_2SiO_4 join, as shown in Fig. 1.

The resulting phase diagram is internally consistent thermodynamically and is consistent with the available calorimetric, thermoelastic and synthesis data, within their experimental uncertainties. Note that the $\alpha+\beta$ divariant loop is extremely narrow, ~2 kbar wide, so that the $\alpha \rightarrow \beta$ transition in mantle olivine would be quite sharp, occurring over a depth interval of ~6 km. The width of this transition is extremely robust to uncertainties in the data set; extreme perturbations of the various parameters yield a variation in transition width of only ±1 kbar (~3 km).

Using the method of free-energy minimization[24], we have calculated stable phase assemblages and associated (Voigt-Reuss-Hill averaged[25]) bulk sound velocities ($\sqrt{\Phi}$) as functions of pressure (depth) along 1,700 K and 2,000 K isotherms for a model mantle consisting of pure olivine of $(Mg_{0.9}Fe_{0.1})_2SiO_4$ composition (Fig. 2a). The model bulk sound velocities for a pure olivine mantle agree quite well (within ±0.06 km s^{-1}) with those calculated from the representative high-resolution P-wave and S-wave velocity profiles GCA[9] (Gulf of California) and TNA[10] (Tectonic North America), respectively. (As we are not attempting to model the 670-km discontinuity, we have not included the effects of any higher pressure phases, such as the silicate perovskite, which might contribute to velocity increases at that depth[2].) A sharp jump in velocity occurs at ~400 km depth due to the $\alpha \rightarrow \beta$ transition. A small kink in the velocity profile occurs at ~550 km due to the $\beta \rightarrow \gamma$ transition, but this slight velocity change is barely detectable due to the similarities of the elastic properties of the β and γ phases[16]. The ratio of the magnitude of the observed (GCA+TNA) velocity increase at 400 km (4.9%) to that calculated for the model pure olivine mantle (6.6%) suggests that the mantle in the transition zone contains ~74% olivine.

We have separated our values of bulk sound velocity ($\sqrt{\Phi}$) into P- and S-wave velocities for a model pure olivine $(Mg_{0.9}Fe_{0.1})_2SiO_4$ mantle (Fig. 2*b*). This requires additional assumptions because the temperature and pressure derivatives of the shear moduli of the high-pressure polymorphs are unknown[26]. To perform the decomposition, we first computed velocities by assuming that the behaviour of the shear moduli at high pressures and temperatures follows the same pattern as that of the bulk moduli, namely that the pressure derivatives and the logarithmic temperature derivatives, respectively, are the same[22] for all the phases of a given component. In a second approach, we followed previous workers[27] in extracting P- and S-wave velocities by assuming that Poisson's ratio for our model pure olivine mantle was the same, at corresponding depths, as that observed (GCA+TNA) seismically. These independent approaches yielded virtually identical results and provide support for our conclusions. The magnitudes of the observed (GCA+TNA) velocity increases at 400 km (4.8 and 4.5% in P- and S-wave velocity, respectively), and those calculated for the model pure olivine mantle (7.2 and 8.1%), are indicative of a mantle composed of ~62% olivine (a peridotitic mantle), in excellent agreement with the results of Weidner[6].

Thus, an isochemical phase change from α-olivine to β-modified-spinel in olivine of mantle composition would produce a sharp 400-km seismic discontinuity ~6 km wide. In fact, our computed velocity increase is even sharper than that required by current seismic observations. The actual sharpness of this discontinuity is difficult to resolve seismically[28,29]. Leven[30] suggests that the discontinuity occurs over a depth interval of ~6 km; other studies[31] suggest that the discontinuity is at least 10 km wide. Our transition width of 6(±3) km is computed for isothermal conditions; temperature gradients through the transition could broaden the discontinuity[4] by up to ~7 km.

Thus, seismic velocities above and below a 400 km depth for a model mantle consisting of pure olivine of $(Mg_{0.9}Fe_{0.1})_2SiO_4$ composition are in good agreement with those observed seismically[9,10]. The magnitudes of the abrupt increases in bulk sound velocity and in P- and S-wave velocities at 400 km are consistent with a mantle composed of between 62 and 74% olivine. Since phase transformations from pyroxene to garnet would not produce such a discontinuity[11], a mantle dominated compositionally by olivine appears necessary for the generation of a sharp 400-km discontinuity unless arbitrary changes in bulk chemical composition are invoked. We therefore conclude that seismic observations are consistent with a periodotitic mantle to a depth of at least 650 km and thus do not require the transition region to be chemically distinct from the overlying mantle.

We thank Jim Leven and Hiroshi Sawamoto for providing preprints of papers before publication. We also thank Ray Jeanloz for providing experimental data from the dissertation of Kawada[13], Masaki Akaogi for critical comments, and Don L. Anderson, Jay Bass, Seth Stein and Emile Okal for helpful discussions. This material is based upon work supported under a NSF Graduate Fellowship (to C.R.B.) and NSF grant EAR-8416793 (to B.J.W.).

Received 23 April; accepted 20 August 1986.

1. Bernal, J. D. *Observatory* **59**, 268 (1936).
2. Ringwood, A. E. *Composition and Petrology of the Earth's Mantle* (McGraw-Hill, New York, 1975).
3. Liu, L. in *The Earth: Its Origin, Structure and Evolution* (ed. McElhinny, M. W.) 177-202 (Academic, New York, 1979).
4. Jeanloz, R. & Thompson, A. B. *Rev. Geophys. Space Phys.* **21**, 51-74 (1983).
5. Navrotsky, A. & Akaogi, M. *J. geophys. Res.* **89**, 10135-10140 (1984).
6. Weidner, D. J. *Geophys. Res. Lett.* **12**, 417-420 (1985).
7. Bass, J. D. & Anderson, D. L. *Geophys. Res. Lett.* **11**, 237-240 (1984).
8. Anderson, D. L. & Bass, J. D. *Nature* **320**, 321-328 (1986).
9. Walck, M. C. *Geophys. R. R. astr. Soc.* **76**, 697-723 (1984).
10. Grand, S. P. & Helmberger, D. V. *Geophys. J. R. ast. Soc.* **76**, 399-438 (1984).
11. Bina, C. R. & Wood, B. J. *Geophys. Res. Lett.* **11**, 955-958 (1984).
12. Suito, K. in *High Pressure Research—Applications to Geophysics* (eds Manghnani, M. H. & Akimoto, S.) 255-266 (Academic, New York, 1977).
13. Kawada, K. thesis, Univ. Tokyo (1977).
14. Sawamoto, H. *Phys. Chem. Miner.* **13**, 1-10 (1986).
15. Watanabe, H. in *High Pressure Research in Geophysics* (eds Akimoto, S. & Manghnani, M. H.) 441-464 (Center for Academic Publications, Tokyo, 1982).
16. Weidner, D. J., Sawamoto, H., Sasaki, S. & Kumazawa, M. *J. geophys. Res.* **89**, 7852-7860 (1984).
17. Wood, B. J. & Kleppa, O. J. *Geochim. cosmochim. Acta* **45**, 529-534 (1981).
18. Akimoto, S. & Fujisawa, H. *J. geophys. Res.* **73**, 1467-1479 (1968).
19. Ringwood, A. E. & Major, A. *Phys. Earth planet. Inter.* **3**, 89-108 (1970).
20. Yagi, T., Bell, P. M. & Mao, H.-K. *Yb. Carnegie Inst. Wash.* **78**, 614-618 (1979).
21. Bina, C. R. & Wood, B. J. *J. geophys. Res.* (submitted).
22. Anderson, O. L., Schreiber, E., Liebermann, R. C. & Soga, N. *Rev. Geophys. Space Phys.* **6**, 491-524 (1968).
23. Birch, F. *J. geophys. Res.* **57**, 227-286 (1952).
24. Wood, B. J. & Holloway, J. R. *Geochim. cosmochim. Acta* **48**, 159-176 (1984).
25. Watt, J. P., Davies, G. F. & O'Connell, R. J. *Rev. Geophys. Space Phys.* **14**, 541-563 (1976).
26. Sumino, Y. & Anderson, O. L. in *CRC Handbook of Physical Properties of Rocks* Vol. III (ed. Carmichael, R. S.) 39-138 (CRC, Boca Raton, 1984).
27. Lees, A. C., Bukowinski, M. S. T. & Jeanloz, R. *J. geophys. Res.* **88**, 8145-8159 (1983).
28. Muirhead, K. *J. geophys. Res.* **90**, 2057-2059 (1985).
29. Ingate, S. F., Ha, J. & Muirhead, K. J. *Geophys. J.R. astr. Soc.* **86**, 57-61 (1986).
30. Leven, J. H. *Phys. Earth planet. Inter.* **38**, 9-27 (1985).
31. Silver, P. G., Carlson, R. W., Bell, P. & Olsen, P. *Eos* **66**, 1193-1198 (1985).

Natural and anthropogenic causes of lake acidification in Nova Scotia

Eville Gorham*, John K. Underwood†, Frank B. Martin‡ & J. Gordon Ogden III§

* Department of Ecology and Behavioral Biology, University of Minnesota, Minneapolis, Minnesota 55455, USA
† Nova Scotia Department of Environment, Halifax, Nova Scotia B3J 3B7, Canada
‡ Statistical Center, University of Minnesota, Saint Paul, Minnesota 55108, USA
§ Department of Biology, Dalhousie University, Halifax, Nova Scotia B3H 4J1, Canada

Controversy has arisen over the recent acidification of lakes[1-4], ascribed by many to anthropogenic acid deposition from the atmosphere[5,6], and by some to natural processes of soil acidification enhanced by the regrowth of forests after cutting and burning[7-10]. Here we show, by analysing the chemistry of Nova Scotian lakes and ponds on base-poor terrains, that both anthropogenic and natural acidification can be important. We calculated correlations and regressions between hydrogen ion (H^+) concentrations and each of four predictors: dissolved organic carbon (DOC) (a surrogate for complex coloured organic acids, often of high molecular weight[11,12]), non-marine sulphate (denoted by the prefixed asterisk as $*SO_4^{2-}$; a surrogate for acid deposition[13]), non-marine calcium ($*Ca^{2+}$; the major basic cation from soil weathering and ion exchange), and the sum of the other non-marine base cations sodium, magnesium and potassium ($*(Na^+ + Mg^{2+} + K^+)$). The results indicate that acidity in these waters is affected both by organic acids from peatland catchments and by acid deposition from long-range and local sources (see ref. 14).

Previous investigators ascribed acidity of lakes on diverse geological substrates in Halifax County to either peaty inflows[15] or acid deposition[16]. Both used methods inadequate for measuring SO_4^{2-} in coloured waters[17], so another study was needed. We sampled lakes on granite and quartzite terrains between 2.5 and 42 km around the Halifax-Dartmouth power plant, whose annual emissions declined from 21.5 kton SO_2 in 1980 to 8.3 kton in 1984 (ref. 18). Thirty-seven surface waters were collected during 7-18 December 1984 after a dry period (September-November precipitation, 42% normal) and filtered through Reeve-Angel no. 934AH glass-fibre filters before analysis. H^+ was measured by a Radiometer combination electrode, DOC by photo-oxidation, gas dialysis and colorimetric titration with phenolphthalein, and Ca^{2+}, Mg^{2+}, Na^+ and K^+ by atomic absorption spectrophotometry. SO_4^{2-} was analysed by ion chromatography and colorimetrically by methyl thymol blue after photo-oxidation; results were averaged. (Ion chromatography yielded a mean 1.2% above that of colorimetry, r^2 was 0.97, the slope of the relation departed by only 2.5% from the 1:1 line, and the average difference between techniques was 6 μequiv.$^{-1}$.) $*SO_4^{2-}$, $*Ca^{2+}$ and $*(Na^+ + Mg^{2+} + K^+)$ were estimated as differences between total and marine concentrations, the latter from ratios to chloride (Cl^-) in sea water. Cl^- was measured by ion chromatography and colorimetrically by mercuric thiocyanate; results were averaged. (Colorimetry yielded a mean 1.4% above that of ion chromatography, r^2 was 0.99, but the slope of the relation departed from the 1.1 line by 8%, so that at very low concentrations colorimetric values were 15% below those of ion chromatography, whereas at very high concentrations colorimetric values exceeded those of ion chromatography by almost 5%. Average difference between techniques was 17 μequiv.$^{-1}$). Colour was measured as absorbance at 320 nm in a 1-cm cell (A_{320}^{1cm}), and in Pt/Co units. Because of plant uptake and microbial reduction, nitrate and ammonium ions—important components of acid deposition—were negligible (N usually <0.01 mg l^{-1}). Alkalinity was usually <2 and always <25 μequiv. l^{-1}. Ranges of chemical properties were: DOC, 0.7-27 mg l^{-1}; colour (A_{320}^{1cm}), 0.001-0.574 and (Pt/Co units), 7-200; H^+, 1-98 μequiv. l^{-1}; Cl^-, 90-832 μequiv. l^{-1}; $*SO_4^{2-}$, 12-203 μequiv. l^{-1}; $*Ca^{2+}$, 17-239 μequiv. l^{-1}; and $*(Na^- + Mg^{2+} + K^+)$, 2.4-105 μequiv. l^{-1}. In the last case, mean percentages were: $*Na^+$, 64; $*Mg^{2+}$, 23; $*K^+$, 13.

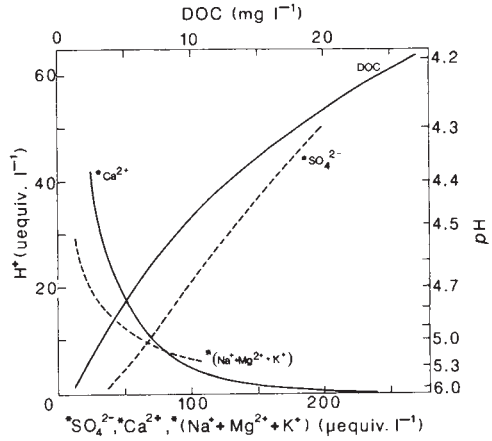

Fig. 1 Partial regressions of H^+ on DOC, $*SO_4^{2-}$, $*Ca^{2+}$ and $*(Na^+ + Mg^{2+} + K^+)$.

We analysed the chemistry of 33 waters statistically, excluding four lakes by standard diagnostic criteria for regressions[19]. Data were transformed to linearize relationships between H^+ and the predictors; error distributions were also normalized. H^+ was transformed to its square root, other data to natural logarithms. Transformed means were: H^+, 3.93; DOC, 1.50; $*SO_4^{2-}$, 4.43; $*Ca^{2+}$, 4.03; and $*(Na^+ + Mg^{2+} + K^+)$, 3.60.

In the transformed scales, DOC is the best of the four predictors of H^+: its correlation coefficient is 0.746 and its partial correlation coefficient—in an equation including $*SO_4^{2-}$, $*Ca^{2+}$ and $*(Na^+ + Mg^{2+} + K^+)$—is 0.908. (Except where specified, all correlation coefficients are significant at $p < 0.01$.) For $*SO_4^{2-}$ the corresponding statistics are lower, with a correlation